Interactions of 85-Mev Positive Pions with Deuterons*†

KENNETH C. ROGERS‡§ AND LEON M. LEDERMAN
Nevis Cyclotron Laboratory, Columbia University, Irvington-on-Hudson, New York
(Received June 12, 1956)

Collision processes of pions with deuterium have been observed in a diffusion cloud chamber. The use of positive pions rendered visible all of the possible reactions at 85 Mev. Total cross sections and angular distributions for elastic and inelastic scattering, charge exchange scattering, and absorption have been determined from 272 collisions in the deuterium gas. The results are compared with the phenomenological impulse-approximation theory.

I. INTRODUCTION

THE experimental approach to meson scattering in deuterium has been stimulated by several circumstances. There exists, in the impulse approximation, a promising theoretical attempt to treat three- (and more-) body collisions on the basis of experimentally known two-body interactions. A crucial and fundamentally interesting assumption in this theory is that the two-body scattering interaction is not modified by the presence of another particle bound by nuclear force to the struck nucleon. The extensive study of pion scattering on protons has progressed to a point where the phenomena are conveniently described by a set of phase shifts known with varying precision up to about 200 Mev. Thus the general behavior of the two-body reactions $\pi^+ + p$, $\pi^- + p$, and (by charge symmetry) $\pi^+ + n$ is well known, with every expectation that new experiments will soon result in much increased precision. A critical test of the assumptions and conditions of validity of the theory is, in principle, the scattering of pions in deuterium.

Pions may interact with deuterons in five possible ways:

(1a) $\pi^+ + d \rightarrow \pi^+ + d$ (elastic scattering),

(1b) $\pi^+ + d \rightarrow \pi^+ + n + p$ (inelastic scattering),

(2) $\pi^+ + d \rightarrow \pi^0 + p + p$ (charge exchange scattering),

(3) $\pi^+ + d \rightarrow \gamma + p + p$ (radiative absorption),

(4) $\pi^+ + d \rightarrow p + p$ (nonradiative absorption).

The corresponding negative-pion interactions can be derived from the above set by interchanging p and n. The principle of charge symmetry requires that the interactions of positive and negative pions with deuterons be the same, except for Coulomb effects which constitute a small correction to the nuclear interactions for fast pions. By using scintillation counter techniques, deuterium total cross section determinations have been performed for both positive and negative pions at a variety of energies.[1–4] A measurement of elastic pion-deuteron scattering at 140 Mev using heavy-water-loaded emulsions but with low statistical precision has been reported.[5] However, with the exception of the work of Nagle at 119 Mev, investigation of the cross sections and angular distributions for the individual processes giving rise to the total deuterium cross section has not previously been carried out. The transmission measurements have tended to indicate that the deuterium total cross section is less than the sum of the scattering cross sections for positive and negative pions by protons, with a maximum difference between the deuterium cross section and the free-nucleon sum occurring at energies in the neighborhood of the first maximum in the free-nucleon cross sections, i.e., at ~200-Mev laboratory kinetic energy. The most critical test of a theory of pion-deuteron scattering requires a determination of the differential and total cross sections for each of the possible pion-deuteron reactions. The following paper describes the determination of the partial and differential cross sections for the processes 1a, 1b, 2, 3, and 4 at a laboratory kinetic energy of 85 Mev, the highest positive-pion beam energy available at this laboratory. A positive-pion beam was chosen in order to permit separate identification of processes 2, 3, and 4.

II. EXPERIMENTAL METHOD

A major technical difficulty associated with the performance of a diffusion cloud chamber experiment using deuterium as a target gas is that of obtaining a sufficient quantity of essentially tritium-free deuterium. The β activity of tritons present in the filling gas places a constant ionization load on the chamber. One triton decay per second per cubic centimeter of filling gas would probably disrupt satisfactory operation of the

* This research is supported in part by the joint program of the Office of Naval Research and the U. S. Atomic Energy Commission.

† A preliminary report of this research appears in the Proceedings of the CERN Symposium, CERN, Geneva, 1955.

‡ Submitted by Kenneth C. Rogers in partial fulfillment of the requirements for the degree of Doctor of Philosophy in the Faculty of Pure Science, Columbia University.

§ Now at Laboratory of Nuclear Studies, Cornell University, Ithaca, New York.

[1] H. A. Bethe and F. de Hoffmann, *Mesons and Fields* (Row, Peterson and Company, Evanston, 1955), Vol. II. This reference lists all work on $\pi - d$ total cross sections published prior to 1955.

[2] Ashkin, Blaser, Feiner, Gorman, and Stern, Phys. Rev. **96**, 1104 (1954).

[3] D. E. Nagle, Phys. Rev. **97**, 480 (1955).

[4] Ignatenko, Moukin, Ozero, and Pontecorvo, Doklady Akad. Nauk S.S.S.R. **103**, 209 (1955).

[5] Arse, Goldhaber, and Goldhaber, Phys. Rev. **90**, 160 (1953).

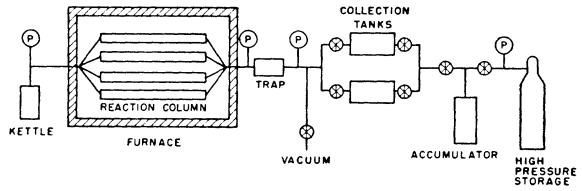

FIG. 1. Flow sheet for $D_2O \rightarrow D_2$ system.

chamber. Under normal conditions the chamber should operate with deuterium at on optimum pressure of 18 atmospheres.[6] The 12-year triton mean life together with the above requirements then establishes a lower limit of approximately 10^{12} for the permissible deuteron-to-triton ratio present in the filling gas. Naturally occurring deuteron-to-triton ratios in water range from 10^{11}, to 10^{12}.[7,8] Thus, under favorable circumstances it should be possible to obtain a sample of deuterium satisfying this requirement. Commercially available deuterium proved to contain far too much tritium for diffusion cloud chamber use. Fortunately a sufficient quantity of heavy water of low tritium content was obtained from the U. S. Atomic Energy Commission. The conversion of the deuterium oxide to deuterium gas was effected by means of the reaction: $D_2O+Mg \rightarrow MgO+D_2$. The method has been described by Knowlton and Rossini.[9] The heavy water was converted to steam and passed over hot magnesium turnings[10] at 500°C in an evacuated stainless steel reaction column. The column consisted of four tubes in parallel each of which contained enough magnesium to react with all of the heavy water. The deuterium product was collected and stored at a pressure of 68 atmospheres in a standard steel cylinder. A flow sheet for the conversion process is given in Fig. 1. The accumulator served to transfer the gas from the collection tanks at a pressure of 3 atmos to the cylinder at 68-atmos pressure. Satisfactory operation of the chamber was achieved with this deuterium. The only evidence for the presence of tritium was a slight decrease in the depth of the sensitive volume from that obtained with ordinary hydrogen.

The experimental arrangement is shown in Fig. 2. The 85-Mev positive pion beam of the Nevis cyclotron was deflected by a double-focussing steering magnet into a deuterium-filled (density=0.003 g/cm^3) 17-in. diameter diffusion cloud chamber. Shielding of the chamber against neutron and gamma background radiation was provided by a 3 ft×4 ft×6 ft concrete block pierced by a 10 in.×2.5 in.×4 ft collimating slit. The beam entered through a 0.040-in. stainless steel window and traversed the chamber with an average radius of curvature of 70 cm in the 9000-gauss pulsed magnetic field. A photographic repetition rate of once every ten seconds was employed. A total of 27 000 stereo photographs was taken. Operation of the chamber has been described in detail previously.[11–13]

III. ANALYSIS OF DATA

(A) Flux

One of the primary objectives of this experiment was the measurement of absolute reaction probabilities. To insure accurate and impartial evaluation of the data a strict scanning and flux counting procedure was adopted. Each picture was examined an a flux count performed by at least two independent observers. All pictures of poor quality or containing more than twenty beam tracks were rejected. To be counted as flux a track was required (1) to fall within the acceptable momentum interval, (2) to extrapolate to the entrance window of the chamber, (3) to make less than a 10° angle with the mean beam direction and (4) to cross fiducial marks scribed on a black glass plate resting on the chamber floor. The purpose of the last requirement was to provide a more rigid definition of a "flux track." The momentum acceptance interval was established from a measurement of the beam momentum spectrum. The lower limit was set to exclude a small low-energy

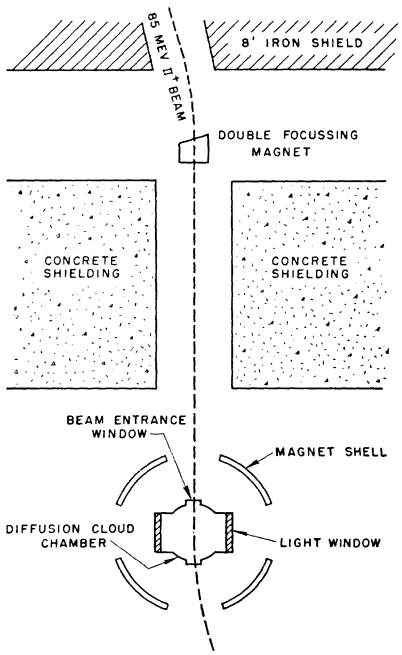

FIG. 2. Experimental arrangement for π^+-d exposure.

[6] R. P. Shutt, Rev. Sci. Instr. **22**, 730 (1951).
[7] I. Kirshenbaum, *Physical Properties and Analysis of Heavy Water* edited by G. M. Murphy and H. C. Urey (McGraw-Hill Book Company, Inc., New York, 1951), National Nuclear Energy Series, Vol. 4A, Div. 3.
[8] E. L. Fireman and D. Schwarzer, Phys. Rev. **94**, 385 (1954).
[9] J. W. Knowlton and F. D. Rossini, J. Research Natl. Bur. Standards **19**, 605 (1937).
[10] Reade Manufacturing Company, Inc., Metal Powder Division, Jersey City, New Jersey.
[11] Sargent, Cornelius, Rinehart, Lederman, and Rogers, Phys. Rev. **98**, 1349 (1955).
[12] Sargent, Rinehart, Rogers, and Lederman, Phys. Rev. **99**, 885 (1955).
[13] Rinehart, Rogers, and Lederman, Phys. Rev. **100**, 883 (1955).

tail in the beam. Only the lower limit was utilized in scanning. A calibrated map measurer was used to convert the flux count to the total beam path length on 2500 pictures composed of 50 picture samples from each of the 50 film loads. Checks of the resulting track-to-path-length conversion by two independent observers agreed to within 2%. On the average the flux track counts of different scanners agreed to within 5%. To provide an additional check of the flux-counting procedure, π-μ decays in flight through projected angles greater than 3° were recorded.

(B) Interaction Energy

The measured momentum spectrum of a random sampling of beam tracks was used to determine the mean beam energy and the beam energy spread. The incident-beam momentum distribution was assumed to be a Gaussian parametrized by a mean momentum μ and a standard deviation s. This analysis led to beam momentum of 175 ± 10 Mev/c. The determination was checked on tracks observed to undergo deuterium interactions. In order to do this, the momentum dependence of the deuterium total cross section at $\sim$85 Mev was estimated from a linear fit to the data of Anderson *et al.*[14] in the neighborhood of 85 Mev, yielding $(1/\sigma)\times(d\sigma/d\mu)=9.7\times10^{-3}$ (Mev/c)$^{-1}$. The observed quantities $\langle p\rangle=180$ Mev/c and $s_{\text{obs}}{}^2=282$ (Mev/c)^2 then yield the mean pion beam momentum $\mu=177\pm10.6$ Mev/c and the corresponding mean pion beam energy $E=85.5\pm8.3$ Mev.

(C) Scattering Events

A total of 267 interactions arising from acceptable beam tracks were recorded. Furthermore, events taking place within one centimeter of the exit wall of the chamber were not counted. The double scanning result of 98% over-all efficiency for observing events was regarded as satisfactory. As an additional check on scanning efficiencies some film was scanned a third time. In general, ionization, range, curvature, and kinematics permitted the identification of each event at sight as either a pion interaction with a deuteron or with a heavy nucleus impurity in the filling gas. In addition, deuterium events could be placed in three categories: (a) elastic and inelastic scattering (processes 1a, 1b), (b) charge exchange scattering and radiative absorption (processes 2 and 3), or (c) absorption (process 4). Elastic and inelastic scatterings were characterized by a scattered charged meson and a visible recoil of at least 1.5-mm range. Charge exchange and radiative absorption events were identified by two uncorrelated, heavily ionizing secondary protons, neither one having more than $\sim$20-Mev kinetic energy. Absorption events were characterized by two fast ($\sim$100-Mev) protons, with a minimum correlation angle of 158°. Detailed momenta and angle measurements were required to further identify a particular interaction. The 1.5-mm recoil range requirement established a 17° cut-off angle for the scattering of pions without exchange of charge in the acceptable momentum interval. The recoil range was determined by the requirement that a recoil track have the appearance of a prong rather than that of a spherical blob. This was necessary in order to avoid confusion between scatterings and π-μ decays with associated delta rays or stray blobs near the decay point. At the lower limit of the acceptable pion momentum interval the maximum π-μ laboratory decay angle is $\sim$15°, so that there is little chance that any π-μ decays with associated blobs would have been mistaken for scatterings.

Whenever possible, the vector momenta of the charged particles involved in an interaction were measured and unless the event was obviously not coplanar the function

$$\mathbf{p}_1\cdot(\mathbf{p}_2\times\mathbf{p}_3)/p_1p_2p_3\equiv\cos\delta$$

was evaluated. The quantity δ is a convenient measure of coplanarity which vanishes when $\mathbf{p}_1$, $\mathbf{p}_2$, and $\mathbf{p}_3$ are coplanar and is invariant to rotations of the coordinate system. Mean precision in coplanarity was $\delta=0.015$ radians. The technique of performing the momenta and angle measurements has been described in a previous paper.[12]

IV. RESULTS

(A) Total Cross Section

The total cross section is given by the relation

$$\sigma=N/(L_\pi n),$$

where N is the number of interactions observed for a

TABLE I. Experimental results.

Observed number of interactions[a]	225
Corrections:	
Scanning efficiency	+4
Hydrogen contamination	−7
Corrected number of interactions	222
Uncorrected flux	17 236
Corrections to flux:	
Magnification	−4%
Gas density	−(2.4±0.5)%
Beam contamination	−(11±4)%
Edge effects	−3%
Filling gas contamination	−(6±0.5)%
	−(26.4±4.5)%
Corrected flux	12 680 g/cm^2
Errors:	
Number of interactions (statistical error)	6.6%
Flux	7%
Corrections to flux	4.5%
Resultant rms error	10.5%

[a] The total number of events observed was 267. However, owing to the rejection of photographs for which the flux count was not reliable, only 225 events were used in the total cross section.

[14] Anderson, Fermi, Nagle, and Yodh, Phys. Rev. **86**, 413 (1952).

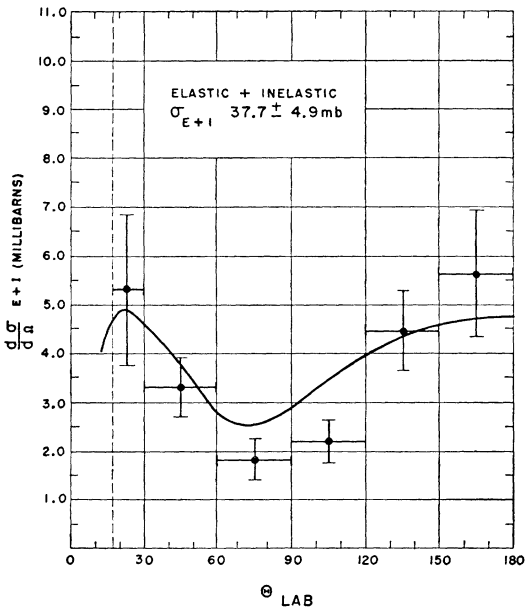

FIG. 3. Elastic plus inelastic differential scattering cross section, $d\sigma_{E+I}/d\Omega$. The experimental points represent 167 events. Errors are standard deviations. The solid line is from Rockmore, using phase shifts of Table II.

pion path length L_π in a target material of n scattering centers per unit volume. The corrections applied to the path length measured in reprojection and to the observed number of interactions are given in detail in Table I. The magnification correction arises because the beam path length measured in reprojection is that for unity magnification in the fiducial plane (the floor of the cloud chamber) and is therefore slightly greater than the true path length in space. The density correction to the perfect gas law was calculated from the b term in the Van der Waals equation of state.[15] The mu-meson and electron contamination of the beam was obtained from range curves taken by various counter groups in this laboratory using the same beam. A calculated correction was made for the difference in geometry. This amounted to $2\pm1\%$. Scatterings which took place outside of a prescribed fiducial area were not counted and a corresponding reduction in the measured flux was applied. Approximately 18% of the film was rejected from the flux count due to poor flux counting conditions, i.e., too many tracks or poor sensitive layer.

A mass spectrographic analysis of the filling gas revealed a 4% hydrogen and 2% nitrogen contamination. These introduced corrections to both the density and the number of events, since pion-proton scatterings could not in general be distinguished from inelastic pion-deuteron interactions. The errors associated with the observed number of events, with the flux count and with the corrections are also tabulated. An independent check of the flux corrections is obtained from the $\pi\rightarrow\mu$ decay count. The number of π-μ decays observed was corrected for (1) scanning efficiency (obtained by comparing the results of the two and three independent observations) and (2) cut-off angle (obtained from the known kinematics). This yields, for 20 selected film loads, a pion path length of 8159 ± 500 g/cm^2 based upon over 2000 events. The error arises primarily from scanning efficiency uncertainties. The direct determination of the path length in these photographs gives 9694 g/cm^2. The difference ($15.6\pm5\%$) represents the magnification, flux contamination, and edge effect corrections to the flux. In Table I, these effects are seen to contribute ($18\pm4\%$). The agreement is considered satisfactory.

No corrections were necessary for events taking place near the top or the bottom of the sensitive volume because the vertical dimension ($\sim$4.5 cm) of the incoming beam was somewhat less than the depth ($\sim$5.5 cm) of the sensitive layer with the mean beam height well centered. An examination of the azimuthal distribution of scatterings with the beam direction taken as azimuth revealed a symmetrical distribution, again indicating no losses through the top or bottom of the sensitive layer or reduction in efficiency for finding scatterings going directly upwards or downwards. Our reported total cross section refers to scatterings without exchange of charge through laboratory angles greater than 17° with no angular restrictions on the remainder of the processes. The resulting total cross section for 85 ± 8 Mev positive pions on deuterons is:

$$\sigma=58.0\pm6.0 \text{ mb}.$$

(B) Elastic and Inelastic Scattering

The energy and momentum conservation laws for elastic scattering correlate the recoil and scattered-

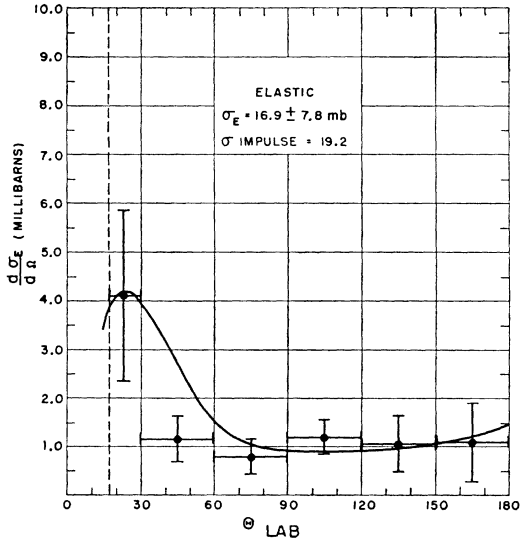

FIG. 4. Elastic differential scattering cross section, $d\sigma_E/d\Omega$. The solid line represents the impulse approximation calculation using phase shifts of Table II.

[15] *Handbook of Chemistry and Physics* (Chemical Rubber Publishing Company, Cleveland, 1955).

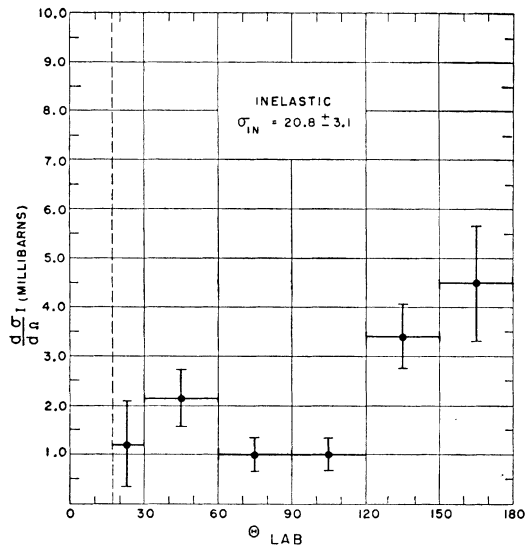

FIG. 5. Inelastic differential scattering cross section, $d\sigma_I/d\Omega$.

particle momenta as well as the recoil and scattering angles for a given incident pion momentum. The identification of a particular event was based on a consideration of how well all of the kinematical requirements (coplanarity, angular correlation, and momentum correlation) were satisfied in view of the assigned measuring errors. The finite depth of the sensitive volume rendered precision measurement of all scatterings impossible. However, the number of events for which a positive identification as elastic or inelastic could be made was sufficiently large to establish within limits the fraction of the scatterings which were elastic, as well as the respective angular distributions. Of the 167 events correctly classified at sight as belonging to category 1*a*, only 13% could not be further identified. The unresolved events have led to an analysis for possible geometrical bias in either of the two angular distributions. The conclusion is that any possible bias would have negligible effect upon the results. The resulting cross sections are, for laboratory scattering angles greater than 17°:

$$\sigma_{E+I}=37.7\pm4.2 \text{ mb},$$
$$\sigma_E=16.9\pm7.8 \text{ mb},$$
$$\sigma_I=20.8\pm3.1 \text{ mb}.$$

The error assigned to the combined elastic and inelastic cross sections includes the statistical error, $[(N+1)^{\frac{1}{2}}/N]\times100\%$, and the error arising from an uncertainty in the beam flux discussed earlier. The large errors assigned to the individual elastic and inelastic cross sections reflect uncertainties in identification and are maximum errors. The observed angular distributions are plotted in Figs. 3, 4, and 5. A search was made to detect distortion of the separate elastic and inelastic angular distributions by those events about which there was some ambiguity. The angular distributions with and without such events were essentially the same. A correction was applied to the inelastic distribution for the 4% hydrogen contamination. An example of an elastic scattering in which the recoil deuteron stopped in the sensitive volume is shown in Fig. 6.

(C) Charge Exchange and Radiative Absorption

Charge exchange and radiative absorption events were identified by the disappearance in flight of the incident pion accompanied by the appearance of two low-energy protons The kinematics of charge exchange scattering and radiative absorption allows the direct determination of the direction, momentum, and energy of the outgoing π^0 or photon if both recoil protons have measurable momentum. In the laboratory reference frame let $\mathbf{P}_1$ be the momentum of the incident π^+ and $\mathbf{P}_0$, $\mathbf{P}_2$, and $\mathbf{P}_3$ be the momenta of the resulting neutral particle and of the accompanying protons, respectively (see Fig. 7). Then, for either charge exchange scattering or for radiative absorption,

$$P_0=(P_1^2+P_2^2+P_3^2-2P_1P_2\cos\Theta_{12}-2P_1P_3\cos\Theta_{13}+2P_2P_3\cos\Theta_{23})^{\frac{1}{2}}$$
$$\cos\Theta_{10}=[P_1-P_2\cos\Theta_{12}-P_3\cos\Theta_{13}]/P_0,$$

where Θ_{10} is the angle between the incident pion and the emerging neutral particle. Conservation of energy then requires that $E_1=T_1+T_2+2M-M_d-E_0$, where E and T denote total and kinetic energies, respectively.

FIG. 6. Diffusion cloud chamber photograph of elastic scattering in deuterium. The incoming beam track is indicated by an arrow. The recoil deuteron comes to rest in the gas.

M and M_d are the proton and deuteron rest energies. Both $\mathbf{P}_2$ and $\mathbf{P}_3$ may not always be directly measurable. However, in general one vector momentum and one vector direction can be measured. In this case the unknown proton momentum can be calculated if a mass is assumed for the neutral particle. Conservation of energy, using this calculated momentum, then provides a consistency check on the validity of the assumption. The conservation laws yield a simple expression for the desired momentum if the protons are treated nonrelativistically and if terms of order $(P/M)^2$ are neglected, where P is the desired proton momentum and M is the proton mass. The result in terms of the known momenta P_1 and P_2 is

$$P_3=\frac{P\cos\delta+\{P\cos^2\delta+[1+(m_0+M)/M](A^2+2m_0A-P^2)\}^{\frac{1}{2}}}{[1+(m_0+A)/M]},$$

where

$$P\cos\delta\equiv P_1\cos\Theta_{13}-P_2\cos\Theta_{23},$$
$$P^2\equiv P_1^2+P_2^2-2P_1P_2\cos\Theta_{12},$$
$$A\equiv m_\pi+T_1-T_2-m_0+M_d-2M,$$
$$m_0\equiv\text{mass of neutral particle (pion or } \gamma \text{ ray}).$$

Of the 60 observed events giving rise to two slow protons, 51 were found to satisfy charge exchange kinematics, 4 to satisfy radiative absorption kinematics, and 5 to satisfy neither. These 5 were assumed to be 2-prong stars from the 2% nitrogen contamination in the filling gas. Thirty two pion stars in flight were observed, corresponding to a nitrogen interaction cross section of 320 ± 53 mb at this energy. This is consistent with what is known about star formation, since the geometric cross section is 355 mb.

The resulting cross sections for charge exchange scattering and for radiative absorption are

$$\sigma_0=12.2\pm2.2 \text{ mb},$$
$$\sigma_\gamma=\ 1.1\pm0.6 \text{ mb}.$$

In Fig. 8 the observed laboratory angular distribution of charge-exchange scattered mesons is plotted. An example of charge-exchange scattering is shown in Fig. 9. Both recoil protons came to rest in the sensitive volume. An example of a charge-exchange scattering followed by the inner pair mode of π^0 decay is shown in Fig. 10.

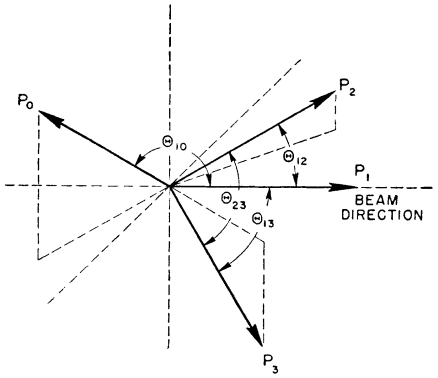

FIG. 7. Charge-exchange vector diagram for $\pi^+ + d \to \pi^0 + p + p$ or $\pi^+ + d \to \gamma + p + p$. P_3 and P_2 are momenta of the recoil protons; P_0 is the momentum of outgoing π^0 meson.

(D) Absorption

As discussed in Part II, interactions arising from the absorption process $(\pi^+ + d \to p + p)$ can be identified at sight. However, all such events were further examined for coplanarity and for angular correlation of the two protons. The space angle between the lines of flight of

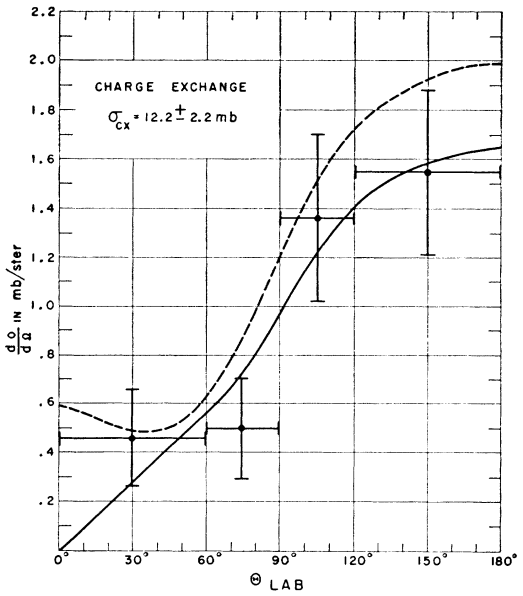

FIG. 8. Charge-exchange differential cross section. The solid line is the impulse approximation result. The dotted curve is the free-nucleon scattering given by the phase shifts in Table II.

the protons and the space angle between the line of flight of each proton and that of the incident pion were required to agree with the kinematically predicted angles. In general the agreement was excellent. The measured total absorption cross section corresponding to 31 events is $\sigma_A=7.0\pm1.4$ mb.

V. DISCUSSION

(A) Elastic and Inelastic Scattering

Several authors[16–20] have discussed pion-deuteron scattering in terms of the phenomenological impulse

[16] Fernbach, Green, and Watson, Phys. Rev. **82**, 980 (1951).
[17] Fernbach, Green, and Watson, Phys. Rev. **84**, 1084 (1951).
[18] Thomas A. Green, Phys. Rev. **90**, 161 (1953).
[19] J. S. Blair, Phys. Rev. **83**, 1246 (1951).
[20] B. Segall, Phys. Rev. **83**, 1247 (1951).

FIG. 9. Diffusion chamber photograph of a charge-exchange scattering in deuterium: $\pi^+ + d \rightarrow \pi^0 + p + p$.

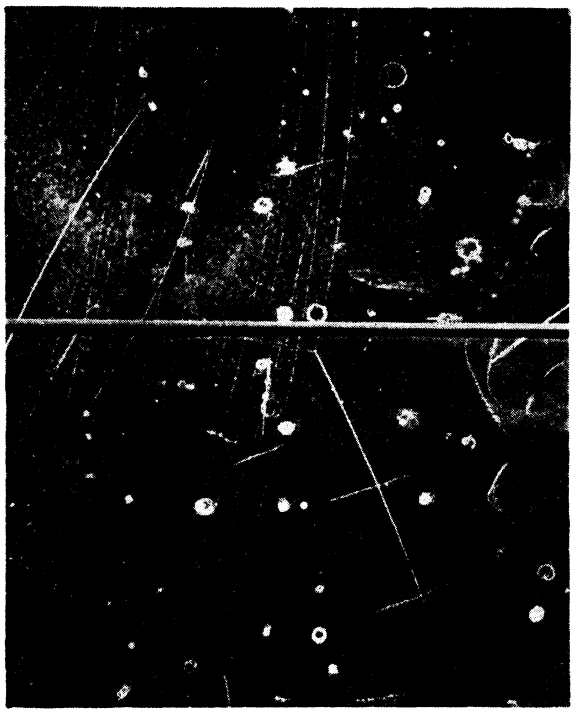

FIG. 10. Diffusion chamber photograph of a charge exchange followed by $\pi^0 \rightarrow \gamma + e^+ + e^-$.

approximation of Chew[21–23] in which the deuteron scattering amplitude is taken to be a linear superposition of the free-nucleon scattering amplitudes. Binding effects on the scattering matrices are neglected as well as off-the-energy-shell dependence of the scattering matrices. The nucleons are considered to scatter as free particles having a momentum distribution characteristic of the deuteron. The scattering is then completely described in terms of the experimentally measured phase shifts for pion-nucleon scattering and the deuteron nucleon momentum distribution. The ratio of elastic to inelastic scattering as well as the angular distributions and energy spectrum of the scattered mesons can all be calculated. The results for combined elastic plus inelastic scattering can be grouped into contributions from individual scatterers plus an interference term which is modulated by the deuterium form factor. The effect of the binding force between nucleons during the scattering, the attenuation of the amplitude of the incident wave in crossing the deuterons, and multiple-scattering effects[24–26] all introduce corrections to the impulse approximation. The loose binding of the deuteron and the fact that it consists of only two nucleons suggest that the multiple scattering corrections will be the most important ones for pion kinetic energies greater than ~50 Mev. A reformulation of the pion-deuteron scattering problem in a fashion to include Coulomb effects and to permit estimation of multiple scattering and binding corrections has been carried out by Rockmore.[27] His results for a pure scattering (no absorption) model in adiabatic approximation for the treatment of the nuclear motion are equivalent to those of Fernbach *et al.*[16,17] with an additional Coulomb correction. In addition, Rockmore finds significant contributions from absorptive scattering and potential corrections which act to decrease the total cross section.

An experimentally determined phase shift solution at 85 Mev for pion-nucleon scattering was not available at the time of this writing. However, the set of phase shifts used in evaluation of the theoretical expressions of Rockmore is given in Table II.

The values of α_1 and α_3 are those obtained by a linear extrapolation from the low-energy slopes given by Orear,[28] i.e., $\tan\alpha_1 = 0.16\eta$, $\tan\alpha_3 = -0.11\eta$, where $\eta = P_\pi c/m_\pi c^2$. The value for α_{33} is that given by Bethe

TABLE II. Phase shifts at 85 Mev.

$\alpha_1 = +9.1°$	$a_3 = -6.8°$	$\alpha_{33} = 15.5°$
$\alpha_{31} = \alpha_{13} = -2.5°$		$\alpha_{11} = 0$

[21] G. F. Chew, Phys. Rev. **80**, 196 (1950).
[22] G. F. Chew and G. C. Wick, Phys. Rev. **85**, 636 (1952).
[23] G. F. Chew and M. L. Goldberger, Phys. Rev. **87**, 778 (1952).
[24] K. Brueckner, Phys. Rev. **89**, 834 (1953).
[25] K. Brueckner, Phys Rev. **90**, 715 (1953).
[26] S. D. Drell and L. Verlet, Phys. Rev. **99**, 849 (1955).
[27] R. Rockmore, Phys. Rev. **104**, 256 (1956), following paper.
[28] J. Orear, Phys. Rev. **100**, 288 (1955).

TABLE III. Experimental and theoretical cross sections, in millibarns; the latter are based upon the phase shifts of Table II.

Reaction	Number of events	Experimental results (mb)	Theory: impulse approximation (mb)	Free nucleon (mb)
Elastic scattering	59	$\sigma_E = 16.9 \pm 7.8$	19.2	$\sigma_{++} = 38.6$
Inelastic scattering	86	$\sigma_I = 20.8 \pm 3.1$		
Ambiguous	22			
Sum	167	$\sigma_{E+I} = 37.7 \pm 4.2$	43.1	41.1
Charge-exchange scattering	51	$\sigma_c = 12.2 \pm 2.2$	12.0	$\sigma_{-0} = 14.6$
Sum	218	$\sigma_{E+I} + \sigma_c = 49.9 \pm 4.7$	55.1	55.7
Sum with corrections to impulse approximation			49.9	
Absorption	31	$\sigma_A = 7.0 \pm 1.4$		
Radiative absorption	4	$\sigma_{RA} = 1.1 \pm 0.6$		
Total cross section		$\sigma = 58.0 \pm 6.0$		

and de Hoffmann.[29,30] The values for α_{31} and α_{13} were taken to be equal and are essentially those values found by Metropolis *et al.*[31] from the data of Steinberger at 65 Mev.[32] The phase shift α_{11} is believed to be small[33] and was arbitrarily set equal to zero. The cross sections calculated from this set of phase shifts as well as the free nucleon cross sections are compared with the observed quantities in Table III. The corresponding differential cross sections are plotted in Figs. 3 and 4. It is to be noted that considerable latitude is allowed by present π-nucleon data in the choice of phase shifts. This is due to the fact that precise experiments are available only at 65 Mev, 120 Mev, and higher. The existence of the "small phase shifts" makes the interpolation even more difficult, since small variations of α_{31} and α_{13} have a large effect upon the resulting best-fit α_{33}. Omission of these phase shifts would require significant changes in α_{33}, α_3, and α_1 to restore a fit to our data, as well as to the 65-Mev π-nucleon data.[31] No attempt has been made here to optimize the fit, the comparison with theory being regarded as provisory, awaiting good π-nucleon data at this energy.

Other experiments[3] at somewhat higher energies have indicated that the simple addition of the free-nucleon cross sections is a fair approximation to the deuterium scattering. This is true of the data of this experiment; see Table III. However, the sum of the free-nucleon cross sections and the results of Rockmore are not very different. The calculated sum, in pure impulse approximation, of elastic and inelastic scattering is somewhat larger than the sum of the free-nucleon cross sections and somewhat larger than the observed sum. The net constructive interference arises from the form factor $H_d(2K)$ and the phase space factor ρ_d/ρ_F which favors the constructive forward interference over the destructive backward interference.[27] This is brought into better agreement with experiment by the absorptive and potential corrections. The corresponding differential cross section agrees qualitatively with the simple impulse calculation. More interesting is the satisfactory agreement of the observed and calculated total and differential cross sections for elastic scattering. The large uncertainties in the measured elastic cross section prevent a critical test of the theory; however, it is clear that the essential features of the elastic scattering are correctly described by the impulse approximation at this energy.

The inelastic scattering was not calculated separately. The observed inelastic differential cross section indicates that most of the inelastic scattering arises from large momentum transfers to the deuteron corresponding to pion scatterings through angles greater than 90°. The reluctance of the deuteron to disintegrate under small momentum transfers has also been observed in *n-d* scattering.

The results reported here indicate that at 85 Mev the gross features of pion-deuteron scattering are correctly given by a straightforward application of the impulse approximation. The work of Brueckner and of Drell and Verlet has indicated that multiple-scattering effects should in general play an important role in pion-deuteron scattering. Multiple scattering is expected to become important when the magnitudes of the free-particle scattering amplitudes are comparable to the mean spacing between the bound nucleons. For large-angle elastic scattering, the two nucleons must be within a distance $R \sim 1/k$ of each other to accept a momentum transfer of order k. As a basis for a simplified discussion following Drell, one can consider only S-wave scattering for which the scattering amplitude has the form

$$f(\mathbf{k},\mathbf{k}') = \sin\delta e^{i\delta}/k, \quad |\mathbf{k}'| = |\mathbf{k}|,$$

where δ is the S-wave phase shift. For multiple scattering to be negligible, $f(\mathbf{k},\mathbf{k}') \ll 1/k$ or $\sin\delta e^{i\delta} \ll 1$. In general, the requirement that the scattering amplitude be small compared to $1/k$ means that all the phase shifts must be small. At 85 Mev this is not true ($\delta_{33} = 0.26$ rad) and multiple-scattering effects should become apparent. Rockmore[27] finds a $+10\%$ correction using the Brueckner model but notes that propagation of the meson wave from one nucleon to another need not conserve energy. This kind of multiple scattering has been studied by Drell and Verlet[26] who find corrections of the order of -10% at these energies, and which are sensitive to the model of off-the-energy shell behavior of the scattering amplitudes.

In view of experimental uncertainties and the lack of precise phase shifts, we can only conclude that, at ~ 85 Mev, the net effect of all of the corrections to the pure impulse approximation amount to $\lesssim 10\%$.

[29] H. A. Bethe and F. de Hoffmann, *Mesons and Fields* (Row, Peterson and Company, Evanston, 1955).
[30] de Hoffmann, Metropolis, Alei, and Bethe, Phys. Rev. **95**, 1586 (1954).
[31] Metropolis, Alei, and Fermi, Phys. Rev. **95**, 1581 (1954).
[32] Bodansky, Sachs, and Steinberger, Phys. Rev. **93**, 1367 (1954).
[33] Friedman, Lee, and Christian, Phys. Rev. **100**, 1494 (1955).

(B) Charge-Exchange Scattering

Previous authors[34–36] have pointed out that deuterium charge-exchange scattering must be less than the free-nucleon charge-exchange scattering despite the fact that charge exchange can take place on only a single nucleon in the deuteron. The diminution in the charge-exchange scattering arises from the requirements of the exclusion principle and parity conservation together with the deuteron momentum distribution. The free-nucleon cross section and the calculated deuterium differential cross section are given in Table III. The charge-exchange destructive interference in deuterium is most readily observed in backward scattering where both the differential cross section and the reduction in the differential cross section over the free nucleon cross section are large. The agreement of the observed and calculated charge exchange scattering near 150° scattering angle indicates that the important features of the destructive interference are properly described on the basis of the impulse approximation. The over-all agreement between the phenomenological theory and experiment is satisfactory.

(C) Absorption

Both the absorption process $\pi^+ + d \rightarrow p + p$ and its inverse, the pion production reaction $p + p \rightarrow \pi^+ + d$, have been studied experimentally at many energies. A bibliography of both the theoretical and experimental work performed before 1954 may be found in papers by Rosenfeld[37] and Stadler.[38] The angular distributions for pion center-of-mass energies up to 94 Mev have been fitted by an expression in the notation of Rosenfeld[37] of the form

$$4\pi\frac{d\sigma}{d\Omega}=\alpha_{10}\eta+\beta_{10}\eta^3\left(\frac{X+\cos^2\theta}{X+\frac{1}{3}}\right),$$

or

$$d\sigma/d\Omega \propto [A+\cos^2\theta],$$

where θ is the center-of-mass angle between the pion and proton directions. Several authors[37,39] have suggested that at low energies,

$$\eta_\pi \ll 1, \quad (\eta_\pi = P_\pi c/m_\pi c^2),$$

A should be proportional to η_π^{-2}. Studies of the absorption process at energies up to 64 Mev have yielded agreement with such an energy dependence. However, experiments[38] at 70 Mev and 94 Mev (center-of-mass system) have indicated that for pion kinetic energies greater than 70 Mev the angular distribution becomes more rather than less isotropic and that the total absorption cross section increases steadily. The absorption and production cross sections can be related by detail balancing if initially unpolarized particles are assumed.

$$\left(\frac{d\sigma}{d\Omega}\right)_{\text{prod}}=\left(\frac{d\sigma}{d\Omega}\right)_{\text{abs}}\left(\frac{3}{4}\frac{k_\pi^2}{k_p^2}\right),$$

where k_π and k_p are the pion and proton barycentric momenta. Pion production studies[40] via the process $p+p \rightarrow \pi^+ + d$ corresponding to pion center-of-mass kinetic energies from 90 Mev to 150 Mev have indicated that the production total cross section possesses a resonance-type behavior, going through a maximum at $\sim$130 Mev, while the angular distribution varies negligibly over the energy range in disagreement with the absorption work at 76 Mev and 94 Mev.

The 31 observed absorption events of this experiment were fitted to a normalized angular distribution of the form

$$\frac{4\pi}{\sigma}\left(\frac{d\sigma}{d\Omega}\right)=\frac{A+\cos^2\theta}{A+\frac{1}{3}}\equiv f(A,\cos^2\theta)$$

by the method of maximum likelihood.[41] If $f(A,\cos^2\theta)$ is an adequate theoretical description of the process, the probability that a given set of points θ_i should have occurred is proportional to Q, where

$$Q\equiv\prod_{i=1}^{31} f(A,\cos^2\theta_i).$$

The maximum likelihood method consists in choosing as an estimate of the parameter A that value which

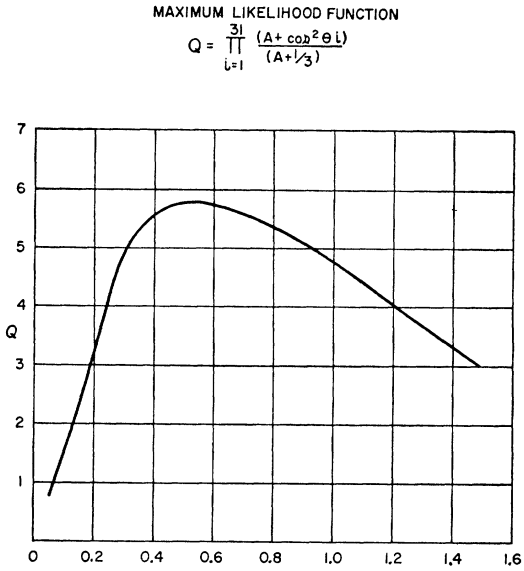

FIG. 11. Plot of the likelihood function $Q(A)$.

[34] R. E. Marshak, Proceedings of the First Annual Rochester Conference on High-Energy Physics, 1950 (unpublished).
[35] W. B. Cheston, Phys. Rev. **83**, 1118 (1951).
[36] Isaacs, Sachs, and Steinberger, Phys. Rev. **85**, 803 (1952).
[37] A. H. Rosenfeld, Phys. Rev. **96**, 139 (1954).
[38] Henry L Stadler, Phys. Rev. **96**, 426 (1954).
[39] K. M. Watson, Phys. Rev. **88**, 1163 (1952).
[40] M. G. Meshcheryakov and B. S. Neganov, Doklady Akad. Nauk S.S.S.R. **100**, 677 (1955).
[41] Harold Cramer, *The Elements of Probability Theory and Some of Its Applications* (John Wiley and Sons, Inc., New York, 1955).

maximizes Q. In Fig. 11 $\ln Q$ is plotted as a function of A. The value of A which maximizes $\ln L$ is seen to be $A=0.50_{-0.31}^{+1.5}$, corresponding to a barycentric kinetic energy of 71 Mev. This result tends to confirm the trend of the angular distribution towards isotropy with increasing energy.

ACKNOWLEDGMENTS

We are indebted to Professor T. I. Taylor of the Columbia University Chemistry department for an analysis of the target gas. Miss Kate Lien, Mrs. Marilyn Schwartz, and Mr. John Impeduglia contributed strongly to the scanning effort.

PHYSICAL REVIEW VOLUME 105, NUMBER 1 JANUARY 1, 1957

Pion-Deuteron Scattering in the Impulse Approximation*†

RONALD M. ROCKMORE‡
Nevis Cyclotron Laboratory, Columbia University, Irvington-on-Hudson, New York
(Received June 12, 1956)

The pure-scattering model of Fernbach, Green, and Watson is used to obtain impulse approximation expressions for the elastic, elastic plus inelastic (closure approximation), and charge-exchange (closure approximation) π-d differential cross sections. The net interference where p-wave scattering is dominant is found to be constructive; the interference due to charge exchange scattering is always negative. The Coulomb effect gives rise to strong destructive interference in the π^+-d elastic component at 85 Mev (laboratory energy of incident pion) for angles $<45°$. The multiple-scattering correction as calculated on Brueckner's model is approximately 10% of the free particle cross section and positive. However, a perturbation field-theoretic treatment of the (3/2, 3/2) double scattering indicates that Brueckner's model is unreliable at low energies. The binding correction to the impulse approximation is calculated using a p-state interaction Hamiltonian (PV coupling) and found to be -3.2 mb at 85 Mev. The forward peak in the elastic differential cross section is found appreciably reduced by destructive interference arising from elastic "absorptive" scattering. It is concluded that, at energies $\lesssim 100$ Mev, absorption corrections are significant, with the multiple-scattering correction becoming important at higher energies.

1. INTRODUCTION

A NEW experiment on the scattering of positive pions by deuterons at 85 Mev, described in detail in the accompanying paper,[1] has motivated the following study of pion-deuteron scattering. In view of the present improved status of the phase shift analysis of pion-nucleon scattering,[2] it is of interest to carry through the method of approach adopted by Fernbach *et al.*[3]: the problem is formulated in terms of the impulse approximation[4] with a phenomenological analysis being made of the leading terms[5] in the expansion of the transition operator for the complex system. In the following, the appellation "usual" impulse approximation is given to these leading terms which form a linear superposition of the two-particle operators referring to the scattering of mesons by single free nucleons. As the work of FGW is essentially independent of any detailed assumptions about the individual scattered amplitudes, their conclusions regarding the use of further simplifying approximations constitute a valid basis for our treatment.

In Sec. 2, the pure-scattering model of FGW is used to derive expressions for the elastic, elastic plus inelastic, and charge exchange ($\pi^+ + d \rightarrow \pi^0 + 2p$) differential cross sections. As the elastic contribution was observed down to 20° in the laboratory, the Coulomb effect is included in the formalism. A general discussion of the properties of these cross sections is given.

The higher order terms[6] in the expansion of the transition operator give rise to the well-known multiple-scattering corrections and the binding or "potential" correction. In Sec. 3 we discuss the first of these, the multiple scattering, from the standpoint of two adiabatic models. We find, using Brueckner's model for multiple scattering,[7] that the total cross section is approximately 10% larger than the total free particle cross section at 85 Mev. Calculations are also presented which indicate large reductions in the total π-d cross section, as well as the elastic differential cross section, at energies in the neighborhood of the pion-nucleon resonance. A qualitative study is also made of the ($t=3/2$, $j=3/2$) multiple scattering at 85 Mev in the double-scattering approximation via a p-state interaction Hamiltonian with pseudovector coupling.

In Sec. 4 the potential correction to the (3/2, 3/2)

* This research is supported in part by the joint program of the Office of Naval Research and the U. S. Atomic Energy Commission.

† Submitted in partial fulfillment of the requirements for the degree of Doctor of Philosophy in the Faculty of Pure Science, Columbia University.

‡ National Science Foundation predoctoral Fellow 1955–1956.

[1] K. Rogers and L. M. Lederman, preceding paper [Phys. Rev. **105**, 247 (1957)], hereafter referred to as Paper I.

[2] J. Orear, Phys. Rev. **100**, 288 (1955).

[3] Fernbach, Green, and Watson, Phys. Rev. **84**, 1084 (1951), hereafter referred to as FGW.

[4] G. Chew and G. Wick, Phys. Rev. **85**, 636 (1952); G. Chew and M. L. Goldberger, Phys. Rev. **87**, 778 (1952).

[5] Chew and Wick, reference 4, Eq. (10); Chew and Goldberger, reference 4, Eqs. (13) and (21).

[6] Chew and Goldberger, reference 4, Eq. (21) and discussion.

[7] K. A. Brueckner, Phys. Rev. **89**, 834 (1953); **90**, 715 (1953).

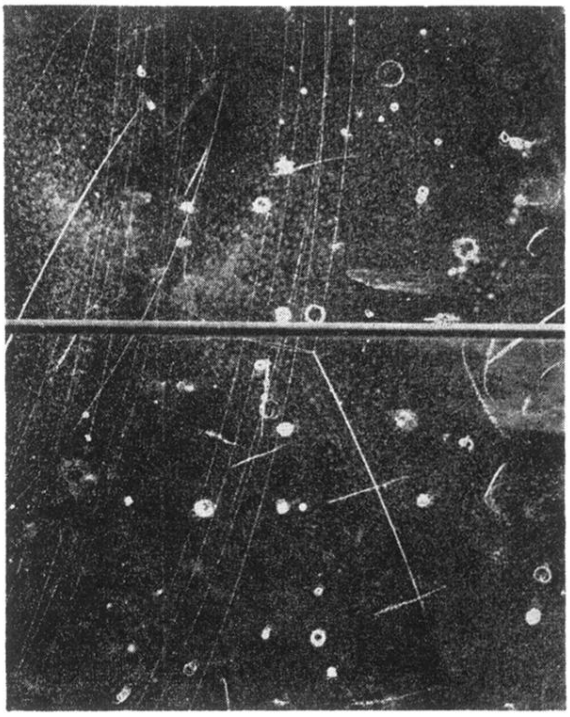

FIG. 10. Diffusion chamber photograph of a charge exchange followed by $\pi^0 \rightarrow \gamma + e^+ + e^-$.

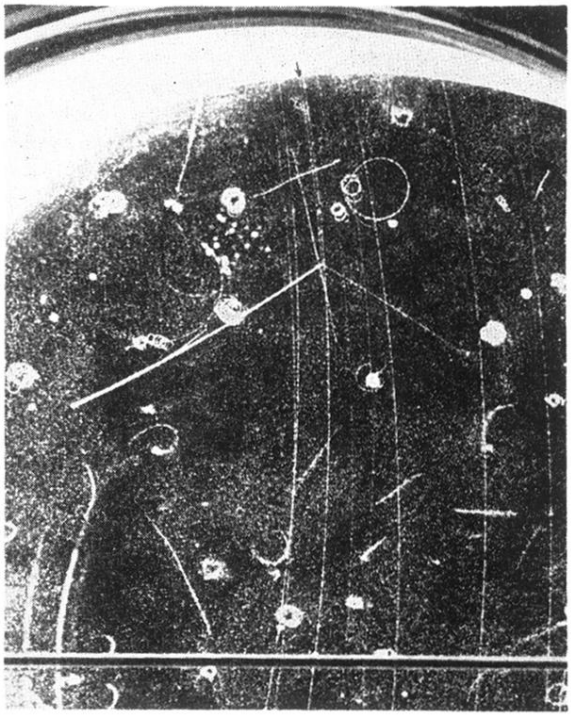

FIG. 6. Diffusion cloud chamber photograph of elastic scattering in deuterium. The incoming beam track is indicated by an arrow. The recoil deuteron comes to rest in the gas.

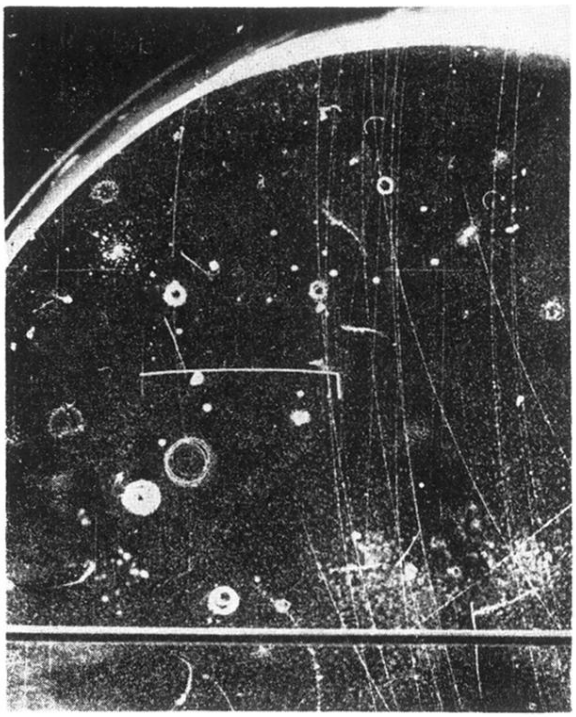

FIG. 9. Diffusion chamber photograph of a charge-exchange scattering in deuterium: $\pi^+ + d \rightarrow \pi^0 + p + p$.